Scanning Microscopy

Volume 1990
Number 4 *Fundamental Electron and Ion Beam Interactions with Solids for Microscopy, Microanalysis, and Microlithography*

Article 18

1990

Slowing Down and Scattering of Ions in Solids

W. Heiland
University of Osnabrück, Germany

H. Derks
University of Osnabrück, Germany

T. Bremer
University of Osnabrück, Germany

Scanning Microscopy Supplement 4, 1990 (Pages 257-263) 0892-953X/90$3.00+.00
Scanning Microscopy International, Chicago (AMF O'Hare), IL 60666 USA

SLOWING DOWN AND SCATTERING OF IONS IN SOLIDS

W. Heiland*, H. Derks and T. Bremer
University of Osnabrück, D-4500 Osnabrück,
W-Germany

Abstract

The interaction of particle beams with solids yields three parts, i.e. reflected particles, penetrating particles and trapped particles. At very low energies particle reflection is dominant, at very high energies penetration is the most important effect. Trapped particles are the result of energy loss processes, which on the other hand cause radiation damage in the solid. In the energy range discussed here, i.e. above energies where quantum effects, diffraction etc. are important and below energies where nuclear reactions, relativistic effects etc. may occur, the particle trajectories are classical. The energy loss process can be treated separately as nuclear and electronic stopping power. The collisions of the projectiles with target atoms are hence binary collisions involving a properly chosen screened Coulomb-potential. In single crystals the structural properties enable channeling, which is a very useful tool in solid state analysis. The electronic stopping includes contributions from single collision processes and collective excitations. Both effects can be described by a dielectric response function. The range of applications covers analytical methods, means to modify solid state properties and also the production of thin films.

Key words: Nuclear Stopping, Electronic Stopping, Surface Channeling, Surface Structure, Ion Scattering Spectrometry, Optical Waveguides, Ion Implantation, Radiation Damage, Secondary Ion Mass Spectrometry, Ion Beam Mixing

*Address for correspondence:
University of Osnabrück
Dept. of Physics
Postfach 4469
D-4500 Osnabrück
W-Germany

Telephon No.: (0)541/608-2675

Introduction

Swift particles interacting with a solid lose their kinetic energy to the nuclei by elastic collisions and to the electrons by a multitude of processes, i.e. elastic collisions, ionisation, plasmon excitation etc. The range of primary kinetic energy considered here excludes nuclear reactions at the high energy side placing the high energy limit to about 1 MeV. By the same token relativistic effects can be neglected too. At low energies, the onset of diffraction effects limits the energy range under consideration that is essentially where the de Broglie wavelength of a particle becomes comparable to a lattice constant (corresponding to less than 1 eV). In a more phenomenological consideration, the energy range can be characterized in terms of reflection and penetration which are the macroscopic manifestation of the particle-particle (projectile ion - target atom) microscopic cross section: The cross section decreases - for e.g. pure coulombic interaction with E^{-2} - with increasing energy such that the particle reflection coefficient varies from about 1 at a few eV to about 0 at 1 MeV, whereas the particle penetration varies from about 0 to 1 consequently. However, there is an increase of the penetration depth too, the range of the particles increases with energy roughly proportional to E. Another qualitative consequence of the variation of the cross section is the change of the probability for large energy transfers in single collisions. At very low energies each projectile is reflected in a single binary collision or in a sequence of very few collisions, hence the energy transfer to the lattice is small. With increasing energy the solid surface becomes 'transparent' and the projectiles lose their energy within a few atomic layers in a series of collisions. At higher energies - decreasing cross section - violent collisions become less probable, i.e. the nuclear energy loss decreases again, since

$$-\frac{dE}{dx} = N\int_o^E \Delta E'\, d\sigma \qquad (1)$$

with N the target atom density, $\Delta E'$ the energy loss in one collision with cross section $d\sigma$ (Fig. 1, Bohr, 1948, Sigmund, 1975, Sigmund, 1981).

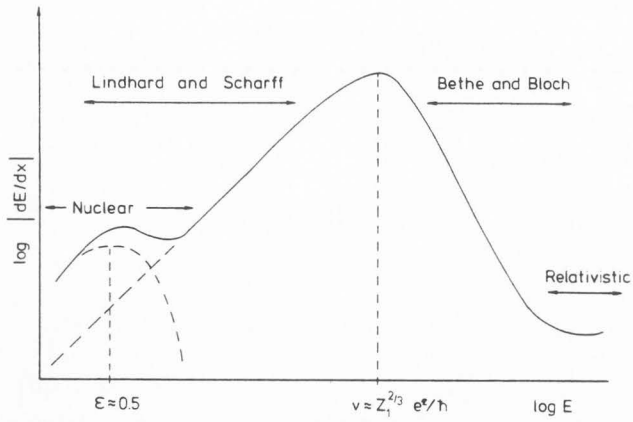

Fig. 1:
Schematic dependence of the stopping power on the particle energy.

$$\varepsilon = \frac{M_2 E}{M_1 + M_2} \frac{a}{Z_1 Z_2 e^2}$$

With target and projectile masses $M_{1,2}$ and atomic numbers $Z_{1,2}$ and the screening length of the potential $a \simeq 0.885\, a_0 (Z_1^{2/3} + Z_2^{2/3})^{-1/2}$ with a_0 = 0.529 Å.

The basis for the behaviour of the electronic stopping with energy is more complex. Qualitatively it can be understood in terms of electron-hole pair excitation and plasmon excitation at the lowest energies, with essentially no threshold for the electron-hole pairs, and thresholds of the order of 10 eV for plasmons. These loss processes increase approximately linearly with velocity v (Lindhard and Scharff, 1961, Lindhard and Winther, 1964). At still higher energies the coupling to the collective properties of the solid decreases. The stopping power is then dominated by ionisation processes: these decrease with energy too as shown more than fifty years ago by Bethe and Bloch (Bethe, 1930, Bloch, 1933). It should be noted that with increasing energy the projectile will be ionized as well, i.e. the actual charge state of the projectile is a function of the energy (Betz, 1983, Echenique et al., 1989). The details of the interactions are target and projectile dependent. Parameters are the mass, the atomic number and the lattice structure, plasmon frequency, dielectric function etc. Phenomena caused by the interactions are sputtering, damage, emission of radiation and of electrons.

Nuclear stopping power

The elastic collision of two particles is described by the differential cross section defined essentially by the impact parameter b:

$$d\sigma = \pi \left| \frac{\partial b^2}{\partial f} \right| df \qquad (2)$$

where $f(\Theta) = \sin^2 \Theta/2$, where Θ is the scattering angle in the center of mass system (c.o.m.). Θ is known from the classical scattering integral

$$\Theta = \pi - 2 \int_{r_{min}}^{\infty} \frac{b/r^2}{(1 - b^2/r^2 - V(r)/E_r)^{1/2}}\, dr \qquad (3)$$

r is the relative coordinate between the particles with masses M_1 and M_2, r_{min} is the distance of closest approach, V(r) the interactomic potential, E_r the kinetic energy.

Obviously, the interatomic potential is a key quantity of the whole field (Torrens, 1972). Presently, screened potentials of the Thomas-Fermi-type (Molière, 1947, Ziegler et al. 1984) and power potentials $V(r) \propto r^{-1/m}$ (Lindhard et al., 1968, Sigmund, 1981) are in use, where m = 1 at high energies and m ≃ 0 at low energies.

The screened potentials in question are given by

$$V(R) = \frac{Z_1 Z_2 e^2}{R}\, \Phi \left(\frac{R}{a} \right) , \qquad (4)$$

with $a = a_0\, 0.88534\, (Z_1^{1/2} + Z_2^{1/2})^{-2/3}$ and Φ_M = 0.35 exp(- 0.3x) + 0.55 exp(- 1.2x) + 0.1 exp(- 6x) and x = R/a for the Molière case (Molière, 1947), and Φ_{ZBL} = 0.1818 exp(- 3.2x) + 0.5099 exp(- 0.9423x) + 0.2802 exp(- 0.4029x) + 0.02817 exp(- 0.2016x) with $a = a_0\, 0.88534 (Z_1^{0.23} + Z_2^{0.23})^{-1}$ for the ZBL case (Ziegler et al. 1984). Since the interaction potential is essentially an empirical quantity, there exists a rich number of different estimates, detailed calculations and averaging methods to obtain useful solutions of the problem (O'Connor and Biersack, 1986).

In order to calculate properties like stopping power and ranges the power potential is a particularly useful approximation, since analytical expressions can be obtained. For the power potential the nuclear stopping cross section $S_n \equiv \int \Delta E d\sigma(E,T)$ becomes

$$S_n(E) = \frac{1}{1-m}\, C_m \gamma^{1-m} E^{1-2m} \qquad (5)$$

with $\gamma = 4\, M_1 M_1\, (M_1 + M_2)^2$ which connects the maximal kinetic energy transfer T_m with the primary energy, i.e. $T_m = \gamma E$, and

$$C_m = \frac{\pi}{2} \lambda_m a^2 (M_1/M_2)^m (2 Z_1 Z_2 e^2/a)^{2m} \qquad (6)$$

where $a = 0.885\, a_0 (Z_1^{2/3} + Z_2^{2/3})^{-1/2}$ with a_0 = 0.529 Å (Bohr's radius) and λ_m a dimensionless function varying slowly with m. S_n shows the energy dependence as in Fig. 1 when m is varied from 0 to 1.

From the nuclear stopping cross section the path length is calculated, neglecting electronic stopping:

$$R_n(E) = \frac{1}{N} \int_{E_{min}}^{E} \frac{dE'}{S_n(E')} \qquad (7)$$

Since the energy of a monoenergetic primary beam will form an energy distribution with increasing penetration into the solid, there will be a range

distribution. In case of implantation, i.e. modification of materials by depositing energetic particles into a solid, the range distribution is called implantation profile, or, if probed by some experimental technique, it is called depth profile.

The damage profile precedes the range profile. It can be calculated by the same formalism as the ranges (Brice, 1975, Winterbon, 1975).

An important aspect of the nuclear stopping is "sputtering" which is discussed in detail by Lam (1990) in these proceedings.

Electronic stopping power

The electronic stopping cross section $S_e(E)$ is defined in analogy to the nuclear term. However, the actual form of $S_e(E)$ depends in a very complex way on the velocity of the particle, its charge and the properties of the solid (Echenique et al., 1986, Echenique et al., 1989).

For high projectile velocities ($v >> Z_1^{2/3} e^2/\hbar$) Bethe (1930) has derived

$$S_e = \frac{4\pi e^4 Z_1^2 Z_2}{m_e v^2} L(v, Z_2), \qquad (8)$$

where m_e is the mass of the electron. In the Bethe-Bloch case $L = \log 2m_e^2/I$, where I is an average ionization potential. For an isotropic Fermi-Gas, Lindhard and Winther (1964) have shown that L can be approximated by

$$L = \frac{i}{\pi \omega_o^2} \cdot \int_o^\infty \frac{dk}{k} \int_{-kv}^{kv} (1/\varepsilon^l(k,\omega) - 1)\ \omega\, d\omega \qquad (9)$$

with $\omega_0 = \sqrt{4\pi e^2 N Z_2/m}$ (plasma frequency), ε^l is the longitudinal dielectric function depent on momentum and frequency. (For details see Echenique et al., 1986, Echenique et al., 1989.)

For low particle energies, i.e. $v << Z_1^{2/3} e^2/\hbar$, an approximate formula for the electronic stopping was proposed by Lindhard and M. Scharff (1961). In agreement with experience the electronic stopping power is proportional to the particle velocity. An extension of the theory has to include the charge state of the moving particle which is a function of the velocity too (Brandt 1982). Hence, more recent theories of the stopping power of low energy particles include necessarily the evaluation of the actual charge state of the moving particle (Echenique et al., 1986, Echenique et al., 1989).

Owing to the practical importance of the electronic stopping, an immense experimental and computational effort has been made to evaluate electronic energy losses for all possible projectile-target combinations. The results have been compiled in the tablework of Andersen (1977), Andersen and Ziegler (1977) and Littmark and Ziegler (1980). These data are the basis for successful implantations and analysis of thin films.

Analysis by ion scattering

The energy of a particle M_1 reflected from a surface atom M_2 has the kinetic energy

$$E_1 = K(\Theta) \cdot E, \qquad (10)$$

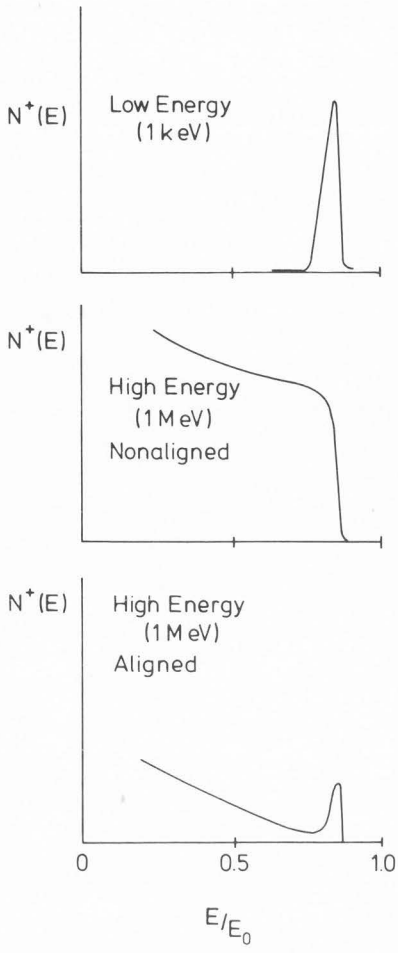

Fig. 2:
Schematic angular resolved energy spectra of ions backscattered from a solid crystal at low energy (top) and high energy (middle, bottom). The middle spectrum is for a random orientation of the crystal. The aligned case (bottom) is achieved by orienting the crystal relative to the beam such that channeling occurs.

where the kinematic factor is given by

$$K(\Theta) = (M_1/(M_2+M_2))^2 (\cos\Theta \pm ((M_2/M_1)^2 - \sin^2\Theta)^{1/2})^2. \qquad (11)$$

Here Θ is the scattering angle in the laboratory system. At low energies (1 keV) backscattered rare gas ions follow eq. 9 with high accuracy (Taglauer and Heiland, 1976, Heiland and Taglauer, 1983). This simple behaviour is partly due to a neutralisation effect which causes particles following multiple scattering trajectories to be neutralised (Jackson et al., 1981). Angular resolved energy analysis affords therefore a very simple tool for the study of the chemical composition of surfaces (Smith, 1967, Taglauer and Heiland, 1976).

With increasing energy, the neutralisation probability for all backscattered particles decreases, such that eventually all reflected particles contribute to the ion spectrum (Fig. 2).

However, for light ions the situation is again relatively simple, since the backscattered particles follow a straight trajectory into the target losing energy by electronic stopping only. Eventually, the projectile makes a large angle in a single collision and leaves the target again on a straight trajectory. The energy spectrum (see e.g. Feldman, 1983) is hence related to the depth t by the yield Y(t)

$$Y(t)\Delta t = (Z_1 Z_2 e^2 / 4 E_t)^2 \; NQ \Delta\Omega \Delta t, \tag{12}$$

where Q is the number of primary particles, $\Delta\Omega$ the solid angle of the detector and

$$E_t = E - t(dE/dx)_E \tag{13}$$

the energy of the projectile at the depth t. For an angle of scattering $\Theta = 180°$ it is

$$dt = dE \quad K((dE/dx)_E + (dE(dx)_{E_1})^{-1} \tag{14}$$

and

$$E_t = (E_1 + AE)/(K+A)$$

with A depending on $(dE/dX)_E/(dE/dX)_{E_t}$. For $K \simeq 1$ and $(dE/dx)_E \simeq (dE/dx)_{E_t}$ the energy spectrum is then

$$N(E_1) \propto \frac{1}{(E+E_1)^2}. \tag{15}$$

The spectrum is schematically shown in Fig. 2 (middle).

In the case of single crystalline samples, channeling effects are observed (Robinson and Oen, 1963, Morgan, 1973, Chu et al., 1978, Feldman, 1983). Under "alignment conditions" (Fig. 2 bottom), a surface peak is observed, the intensity of which represents the backscattering from 1 to 2 atoms per row. It is obvious that these effects can be exploited for the analysis of near surface structure.

Surface Channeling

Compared to bulk channeling, relatively few surface channeling experiments have been reported (Sizmann and Varelas 1976, Schiffner et al., 1977). One reason is the competition of other techniques which are very successful to probe surface structures, i.e. LEED (Low Energy Electron Diffraction) and STM (Scanning Tunneling Microscope) (Davisson and Germer, 1927, Binnig and Rohrer, 1983, Ertl and Küppers, 1985).

Fig. 3 shows as an example a low energy ion scattering result from Au(110) (Derks, 1989). The Au(110) surface forms at room temperature after annealing at about 800K a so-called "missing row" structure which is labelled (1x2) in the usual LEED nomenclature. When heated, a two-dimensional phase transition occurs (Campuzzano et al., 1985) and the LEED patterns shows a (1x1) structure. The phase transition is an order-disorder transition (2D Ising type). In the surface channeling experiment (Fig. 3), the change of the periodicity is manifested by the disappearence of the [114] channel at an azimuthal angle of 74°, whereas the other channels become somewhat flatter only. The narrowing of the [110] channels from the (1x2) to (1x1) structure can be read from the real space pattern of Fig. 3. The disorder of the surface has to be estimated from the minimum yield of the channeling minima. This is quantitatively yet to be done, the problem is the influence of the thermal vibrations of the surface atoms. There are indications that the thermal motion of the surface atoms becomes anharmonic with increasing temperature, i.e. the surface Debye temperature becomes temperature dependent (Derks et al., 1988).

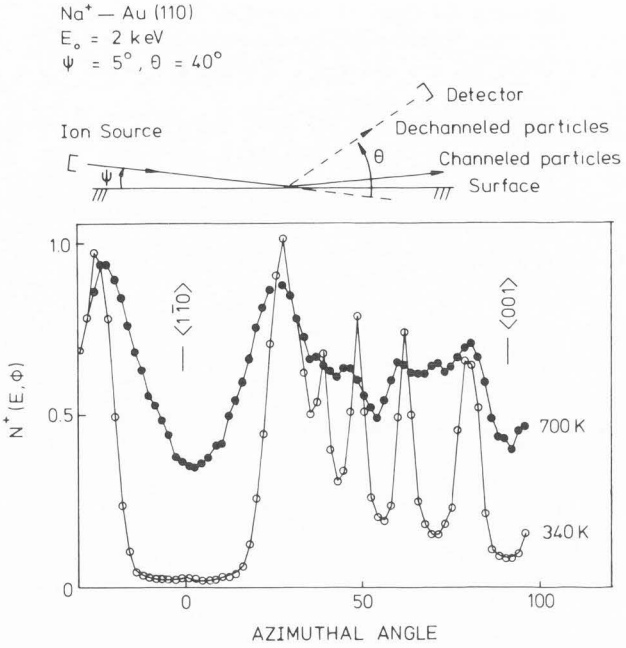

Fig. 3:
Low energy ion backscattering from Au(110) at 340 K and at 700 K. At 650 K Au(110) undergoes a (1x2) ↔ (1x1) phase transition. The two different surface structure are seen here in "surface channeling" patterns.

The application of ion beams for material modification

The literature on ion implantation into solids is abundant (e.g. Brice, 1975,Mayer and Gyulai, 1983). More recently the technique has also been applied to change the refractive index of materials of interest for integrated optical devices, e.g. $LiNbO_3$ or $KNbO_3$ (Destefanis et al., 1978, Bremer et al., 1988a, Bremer, 1989).

In Fig. 4, we compare the ordinary refractive index profiles of He^+ implanted $LiNbO_3$ for different ion energies with the corresponding range distributions calculated by the Monte Carlo computer program TRIM (Biersack and Haggmarck, 1980). The refractive index profiles have been measured by mode spectroscopy and reconstructed with an improved inverse WKB (Wentzel, Kramers, Brillouin) method (Schiff, 1955, Hertel and Menzler, 1987, Bremer et al., 1988b). The decrease of the refractive index is caused by nuclear damage leading to amorphization of the crystal. Thus, the refractive index profiles directly monitor

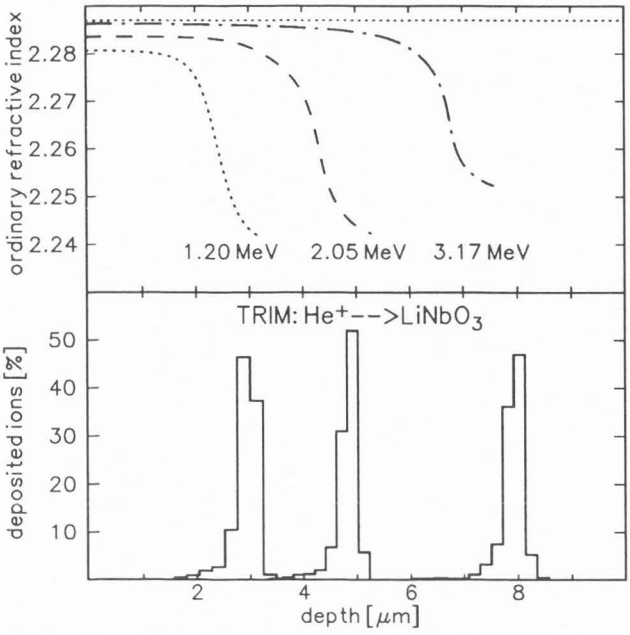

Fig. 4:
Depth distributions of He implanted into $LiNbO_3$ (top) and refractive index profiles caused by the implant (bottom). The refractive index profiles are obtained by measuring the eigenmodes of the planar waveguides formed by the implant and subsequent inverse WKB evaluation.

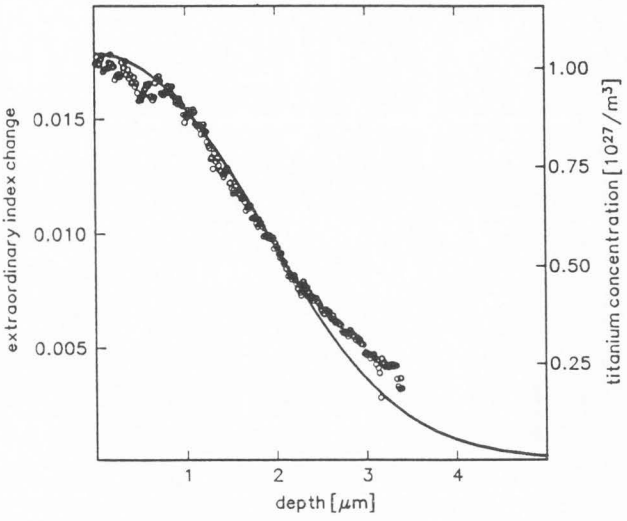

Fig. 5:
Depth distribution of implanted Ti (200 KeV) in $LiNbO_3$ measured by SIMS (dots) and refractive index profile (line) of the planar wave guide formed by the implant. The refractive index profile is evaluated from the measured eigenmodes and an inverse WKB method.

the damage distribution. Below the calculated minimum, the index again increases to the value of the undamaged material, however, this region cannot be explored by an inverse WKB algorithm. Since the damage peak is buried at a depth of a few microns, an optical waveguide is formed between the surface and the region of lowered refractive index. As can be seen from fig. 4, the damage distribution is found at a depth similar to that of the ion distribution, but a small shift towards the surface becomes visible, especially for higher energies.

Besides the nuclear damage distribution, the evaluation of the refractive index profiles also yields information about other effects of ion implantation. This includes electronic damage as well as changes of composition by implanted ions, or ion induced sputtering. In the region of electronic damage between the surface and the amorphized region, the ordinary index is lowered, whereas the extraordinary is raised. These index alterations increase with dose and decrease with ion energy, but are always well below the nuclear damage alterations. Moreover, the electronic damage can be removed almost completely by annealing procedures at moderate temperatures. After such treatments, the remaining alterations near the surface are due to composition changes (alterations in the Li sublattice) which only affect the extraordinary index.

Alternatively to He implantation, refractive index increase can be acieved by implantation of transition metal ions and epitaxial regrowth. Fig. 5 shows an example of Ti implanted $LiNbO_3$ which was produced under the following conditions: 200 keV Ti^+ irradiation at a dose of $2.5 \cdot 10^{17}/cm^2$, subsequently regrown for 8 h at 1000°C in a wet oxygen containing atmosphere. We compare the extraordinary refractive index profile with the Ti concentration profile obtained by SIMS (Secondary Ion Mass Spectrometry). In contrast with the usual diffusion technique, implantation yields shallower profiles and higher local Ti concentrations. In other words, the variety of profiles is not limited by the laws of diffusion and chemical solubility. Also, ion beam mixing of evaporated Ti layers offers a promising attempt for waveguide fabrication (Bremer et al., 1989), However, this technique has not yet been investigated in detail. By ion beam mixing, the Ti is incorporated in the crystal by recoil effects. The proper choice of the irradiation parameters of the incoming Ti beam allows a high mixing efficiency at moderate doses, thus producing less damage to be annealed.

In conclusion, ion beams offer a great potential for the fabrication of waveguides and devices for integrated optics. Using suitable annealing procedures, unwanted side effects of implantation can be removed to a large extent. The optical quality of ion implanted waveguides is comparable to those produced by the classical diffusion technique.

Acknowledgements

We wish to thank D. Kollewe (University of Stuttgart) as well as Ch. Buchal (KFA Jülich) for their assistance with the ion implantation. Financial support by the Deutsche Forschungsgemeinschaft is gratefully acknowledged. Part of the work is performed within the projects A3 and A7 of the SFB 225.

References

Andersen HH. (1977). The Stopping and Ranges of Ions in Matter, Pergamon Press NY, Vol. **2**, 1-207.

Andersen HH, Ziegler JF. (1977). Hydrogen Stopping Powers and Ranges in All Elements, Pergamon Press NY, Vol. **3**, 1-317.

Bethe HA. (1930). Zur Theorie des Durchgangs schneller Korpuskularstrahlen durch Materie, Ann. d. Phys. **5**, 325-400.

Betz HD. (1983). Heavy Ion Charge States, in: Applied Atomic Collision Physics, S. Datz (ed.) Academic Press NY Vol. **4**, 1-42.

Biersack JP, Haggmark LG. (1980). A Monte Carlo computer program for the transport of energetic ions in amorphous targets, Nucl. Instr. Meth. **174**, 257-269.

Binnig G, Rohrer H. (1983). Scanning Tunneling Microscopy, Surf. Sci. **126**, 236-244.

Bloch F. (1933). Zur Bremsung rasch bewegter Teilchen beim Durchgang durch Materie, Ann. d. Phys. **16**, 285-320.

Brandt W. (1982). Effective charges of ions and the stopping power of dense media, Nucl. Instr. Meth. **184**, 13-19.

Bremer T. (1989). Herstellung und Charakterisierung elektrooptischer Wellenleiter durch Ionenbeschuß. Thesis University of Osnabrück.

Bremer T, Heiland W, Hellermann B, Hertel P, Krätzig E, Kollewe D. (1988a). Waveguides in $KNbO_3$ by He^+ Implantation, Ferroelectrics Lett. **9**, 11-14.

Bremer T, Hertel P, Kollewe D. (1988b). Surface Refractive Indices and Profile Widths of He implanted $LiNbO_3$ Waveguides, Nucl. Instr. Meth. **B34**, 62-67.

Bremer T, Kollewe D, Koschmieder H. Heiland W. (1989). SIMS Investigations of Titanium Profiles in $LiNbO_3$ Produced by Ion Beam Mixing and Diffusion, Fresenius Z. Anal. Chem. **333**, 485-487.

Bohr N. (1948). The Penetration of Atomic Particles through Matter, Mat.-Fysiske Meddelelser Kong. Danske Videnskabernes Selskab **18**, 8, 1-144.

Brice DK. (1975). Ion Implantation Range and Energy Deposition Distributions, Plenum Press NY Vol. 1, 1-590.

Campuzzano JC, Foster MS, Jennings G, Willis RF, Unertl W. (1985). The Au(1x2)→(1x1) Phase Transition: A Physical Realization of the 2-D Ising Model, Phys. Rev. Lett. **54**, 2684-87.

Chu W-K, Mayer JW, Nicolet M-A. (1978). Backscattering, Spectrometry, Academic Press, NY.

Davisson LC, Germer LH. (1927). Diffraction of Electrons from a Crystal of Nickel, Phys. Rev. **30**, 705 - 740.

Derks H. (1989). Untersuchungen zur (1x1)⇄(1x2) Phasenumwandlung der Au(110)-Oberfläche. Thesis University of Osnabrück.

Derks H, Möller J, Heiland W. (1988). The Temperature Dependence of the Near Order Structure of Au(110) Studied by Ion Scattering Spectrometry, in: the Structure of Surfaces II. JF van der Veen, MA van Hove (eds.) Springer-Verlag, NY, 496-500.

Destefanis GL, Townsend PD, Gailliard JP. (1978). Optical Waveguides in $LiNbO_3$ formed by ion implantation of helium, Appl. Phys. Lett. **32**, 293-294.

Echenique PM, Nieminen RM, Ashley JC, Ritchie RH. (1986). Nonlinear Stopping Power of an Electron Gas for Slow Ions, Phys. Rev. **A33**, 897-904.

Echenique PM, Flores F, Ritchie RH. (1989). Dynamic Screening of Ions in Condensed Matter, in: Solid State Physics Series, H Ehrenreich, R Seitz D. Turnbull (eds.) Academic Press NY.

Ertl G, Küppers J. (1985). Low Energy Electrons and Surface Chemistry, Verlag Chemie, Weinheim.

Feldman LC. (1983). High Energy Ion Scattering, in: Applied Atomic Collision Physics, S Datz (ed.) Academic Press, NY, **4**, 261-98.

Heiland W, Taglauer E. (1983). Low Energy Ion Scattering and Atomic Diffraction in: Applied Atomic Collision Physics, S Datz (ed.) Academic Press, NY, **4**, 238-260.

Hertel P, Menzler HP. (1987). Improved Inverse WKB Procedure to Reconstruct Refractive Index Profiles in Dielectric Planar Waveguides, Appl. Phys. **B44**, 75-80.

Jackson DP, Heiland W, Taglauer E. (1981). Multiple-Scattering Effects in Ion-Surface Interactions at Low Energies, Phys. Rev. **B24**, 4198-4207.

Lam NQ. (1990). Physical Sputtering of Metallic Systems by Charged Particle impact, Scanning microscopy supplement **4**, pp. 311-352.

Lindhard, J, Scharff M. (1961). Energy Dissipation by Ions in the KeV Region, Phys. Rev. **124**, 128-130.

Lindhard J, Winther A. (1964). Stopping Power of Electron Gas and Equipartition Rule, Mat.-Fysiske Meddelelser Kong. Danske Videnskabernes Selskab **34**,4, 1-21.

Lindhard J. (1964). Influence of Crystal Lattice on Motion of Energetic Charged Particles, Mat.-Fysiske Meddelelser Kong. Danske Videnskabernes Selskab **34**, 14, 1-64.

Lindhard J, Nielsen V, Scharff M. (1968). Approximation Method in Classical Scattering b Screened Coulomb Fields, Mat.-Fysiske Meddelelser Kong. Danske Videnskabernes Selskab **36**, 10, 1-32.

Littmark U, Ziegler JF. (1980) Range Distributions of Energetic Ions in All Elements, Pergamom Press, NY, Vol. **6**, 1-493.

Mayer JW, Gyulai J. (1983). Ion Implantation in Semiconductors in: Applied Atomic Collision Physics S Datz (ed.) Academic Press, NY, **4**, 545-75.

Molière G. (1947). Theorie der Streuung schneller geladener Teilchen I. Einzelstreuung am abgeschirmten Coulombfeld, Z. Naturforschung **2a**, 133-145.

Morgan DV (ed.). (1973). Channeling, Theory, Observation and Applications, J. Wiley & Sons, London.

O'Connor DJ, Biersack JP (1986). Comparison of theoretical and empirical interatomic potentials, Nucl. Instr. Meth. **B15**, 14-19.

Robinson MT, Oen OS. (1963). The Channeling of Energetic Atoms in Crystal Lattices, Appl. Phys. Lett. **2**, 30-32

Schiff LI. (1955). Quantum mechanics. McGraw-Hill, New York, 184-193.

Schiffner R, Goltz K, Varelas C. (1977). Korrelierte Streuung von Ionen an einkristallinen Oberflächen, Vakuum-Technik **26**, 3-8.

Sigmund P. (1975). Energy loss of charged partricles in solids. in: Radiation Damage Pro-

cesses in Materials. Dupuy CHS (ed.) Noordhoff, Leyden, the Netherlands, 3-117.

Sigmund P. (1981). Sputtering by Ion Bombardment: Theoretical Concepts. in: Sputtering by Particle Bombardment I. R Behrisch (ed.) Springer-Verlag, NY, 9-71.

Sizmann R, Varelas C. (1976). Surface Channeling, Nucl. Instr. Meth. **132**, 633-638.

Smith, DP. (1967). Scattering of Low-Energy Noble Gas Ions from Metal Surfaces, J. Appl. Phys. **38**, 340-347.

Taglauer E, Heiland W. (1976). Surface Analysis with Low Energy Ion Scattering, Appl. Phys. **9**, 261-75.

Torrens IM. (1972). Interactomic Potentials, Academic Press, NY, 1-247.

Winterbon KB. (1975). Ion Implantation and Energy Deposition Distributions, Plenum Press, NY, Vol.**2**, 1-341.

Ziegler JF. (1977). Helium: Stopping Powers and Ranges in All Elemental Matter, Pergamon Press, NY, Vol. **4**, 1-367.

Ziegler JF. (1980). Stopping Cross-Sections for Energetic Ions in All Elements, Pergamon Press, NY, Vol. **5**, 1-432.

Ziegler JF, Biersack, JP, Littmark U. (1984). Stopping and Ranges of Ions in Matter. Pergamon Press, NY, 1-321.

Editor's Note: All of the reviewer's concerns were appropriately addressed by text changes, hence there is no Discussion with Reviewers.